SUPPLEMENTAL INFORMATIONS

SUPPLEMENTAL FIGURES

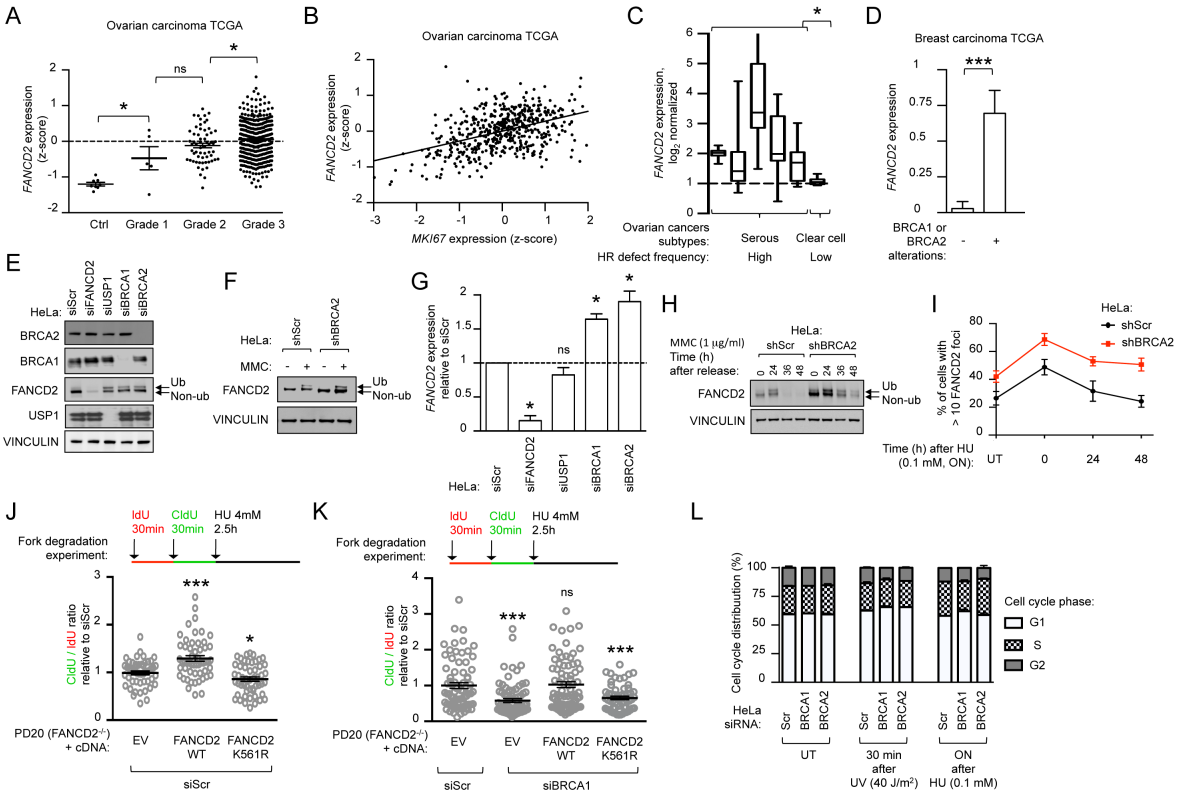

Figure S1. Related to Figure 1. FANCD2 is activated in HR-deficient ovarian and breast tumors. (A-B) *FANCD2* expression correlates with tumor grade (A) and *MKI67* expression (B) in the ovarian TCGA (n=494 patients with ovarian carcinoma (grade 1, n=5; grade 2, n=61; grade 3, n=428) and control samples, n=8). Each dot represents a z-score value for a tumor sample. Data in B were analyzed using the Pearson test (r=0.45, $P<10^{-3}$). (C) *FANCD2* gene expression in 5 data sets of serous epithelial ovarian carcinoma (frequently associated with an HR deficiency) and 1 data set of clear cell ovarian carcinoma (subgroup not associated with HR alterations). For each data set, *FANCD2* expression values are displayed as fold-change differences relative to the mean expression in control samples, which was arbitrarily set to 1. Box plots show twenty-fifth to seventy-fifth percentiles, with lines indicating the median, and whiskers indicating the smallest and largest values. Statistics were used to compare FANCD2 expression in clear cell subtype against each of the other ovarian cancer subtypes. (D) *FANCD2* expression in tumors from the breast TCGA. The presence of alterations in *BRCA1* or *BRCA2* gene is indicated. (E) FANCD2 immunoblot in HeLa cells after siRNA depletion of indicated genes. (F) FANCD2 immunoblot in HeLa cells after shRNA depletion of BRCA2. (G) FANCD2 gene expression analysis (RT-qPCR) in HeLa cells transfected with indicated siRNA. Data is displayed as relative to siScr transfected sample. (H) FANCD2 immunoblot of HeLa cells expressing indicated shRNA at indicated time points after MMC pulse treatment. (I) Kinetic of FANCD2 foci formation in HeLa cells expressing indicated shRNA at indicated time point after a HU pulse treatment. (J, K) Schematic for the labeling of FANCD2-deficient (PD20) cells with IdU and CIdU for fork degradation experiments. Scatter dot plot for CIdU to IdU ratio of cells expressing indicated cDNA and transfected with indicated siRNA. Satistics were performed on n>100 fibers per condition and expressed as relative to EV siScr sample, that was conventionally set to 1. (L) Cell cycle distribution of HeLa cells after siRNA depletion of indicated genes at indicated time point after HU or UV treatment. Data in G, I-L represent mean ± s.e.m. over n=3 independent experiments. Data in A, C-D, G, J-L were analyzed using Student's t test. Abbreviations: ns, non significant; EV, empty vector; WT, wild-type; UT, untreated; ON, over-night.

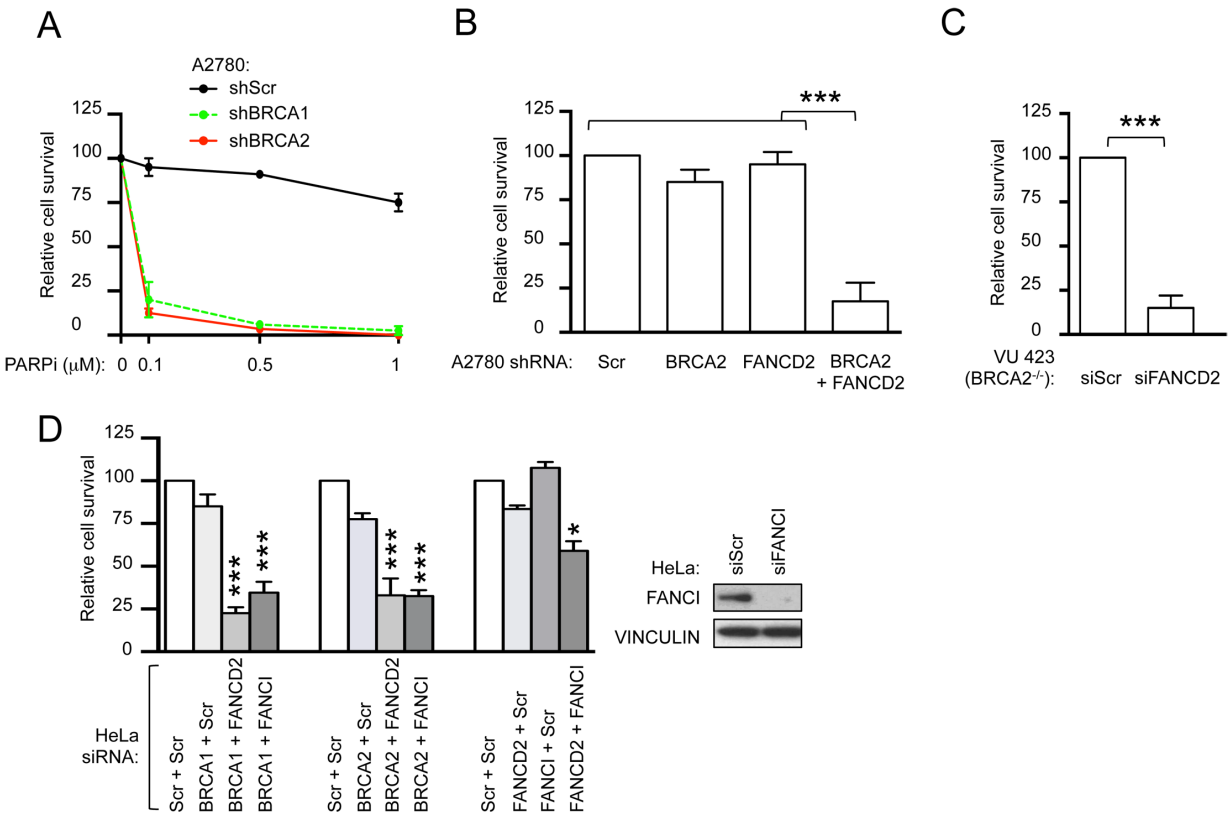

Figure S2. Related to Figure 2. FANCD2 and FANCI are required for survival of BRCA1/2-deficient tumors. (A) Clonogenic formation of A2780 cells expressing indicated shRNA under increasing concentration of PARP inhibitor (PARPi). Percent survival relative to non-treated cells (PARPi 0 μM) is plotted. (B) Clonogenic formation of A2780 cells expressing the indicated shRNA. (C) Clonogenic formation of BRCA2-deficient (VU 423) cells transfected with the indicated siRNA. (D) Clonogenic formation assay of HeLa cells transfected with the indicated siRNA. Data in A-D are displayed as relative to siScr transfected samples, which was arbitrarily set to 100%. Data in A-D represent mean ± s.e.m. over n=3 independent experiments. Data in B-D were analyzed using using the Chi-squared test for trend in proportions.

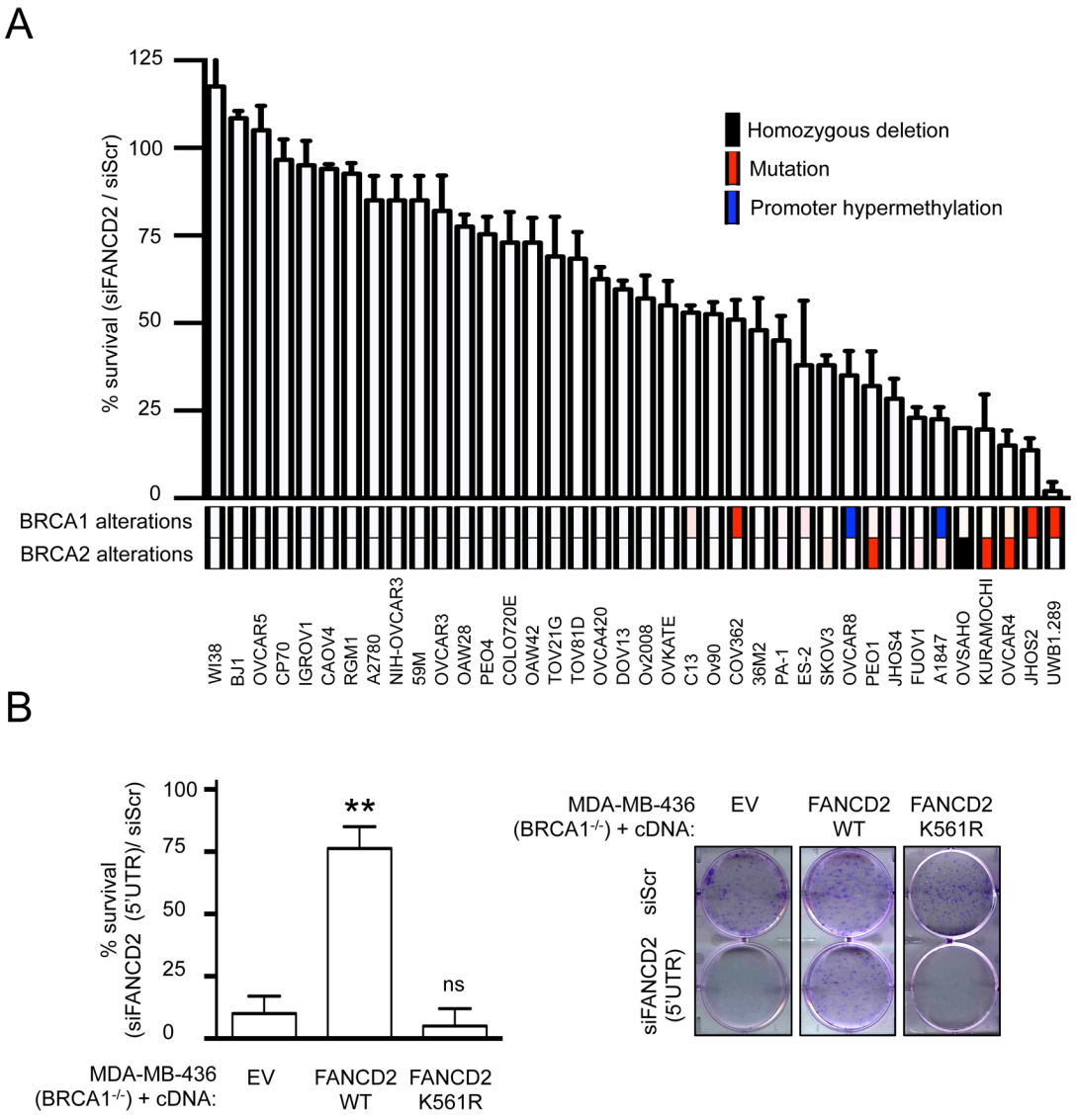

Figure S3. Related to Figure 3. FANCD2 is required for survival of BRCA1/2-deficient ovarian tumors. (A) Clonogenic formation of a panel of 36 ovarian and 2 normal fibroblast cell lines transfected with siScr or siFANCD2. Percent survival of cells transfected with siFANCD2 versus siScr is plotted. The genetic alterations in BRCA1 or BRCA2 genes are indicated. (B) Clonogenic formation of BRCA1-mutated (MDA-MB-436) cells expressing the indicated cDNA constructs and transfected with the indicated siRNA. Survival is expressed as percentage of cells transfected with siFANCD2 (5'UTR) over siScr. Representative images are shown. Data in A-B represent mean ± s.e.m. over n=3 independent experiments and were analyzed using using the Chi-squared test for trend in proportions. Abbreviations: ns, non significant; EV, empty vector; WT, wild-type.

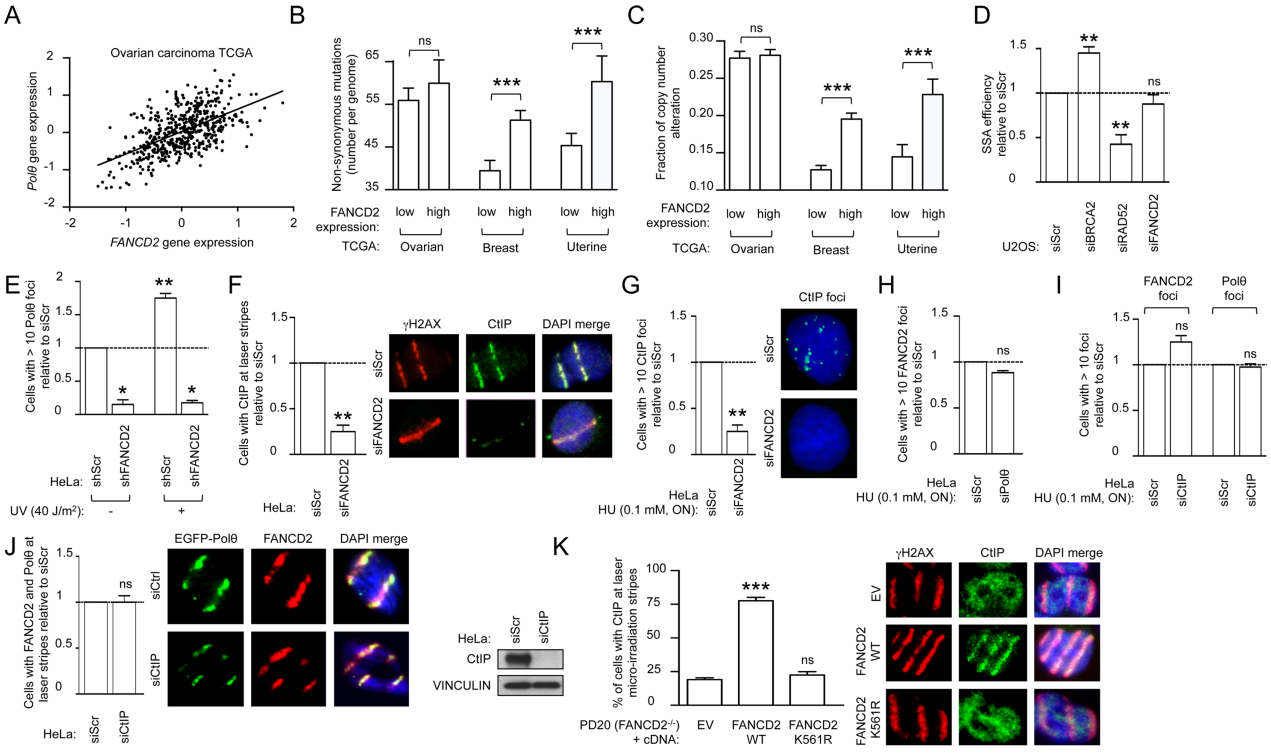

Figure S4. Related to Figure 4. FANCD2 promotes error-prone repair mechanisms. (A) FANCD2 expression correlates with Polθ gene expression in the ovarian TCGA (n=494 patients with ovarian carcinoma (grade 1, n=5; grade 2, n=61; grade 3, n=428) and control samples, n=8). Statistical correlation was assessed using the Pearson test (r=0.58, P <10^{-3}). Non-synonymous mutation count (B) and fraction copy number alteration (C) in ovarian, breast and uterine TCGA. Data represent mean ± s.e.m. (D) Single-strand annealing reporter assay in U2OS cells transfected with the indicated siRNA. (E) Quantification of baseline and damage (UV)-induced Polθ foci in HeLa cells expressing Scr or FANCD2 shRNA. (F) CtIP and γH2AX immunofluorescence in HeLa cells treated with Scr or FANCD2 siRNA after laser micro-irradiation. Representative images are shown. (G) Quantification of damage (HU)-induced CtIP foci in HeLa cells transfected with the indicated siRNA. Representative images are shown. (H) Quantification of damage (HU)-induced FANCD2 foci in HeLa cells transfected with indicated siRNA. (I) Quantification of damage (HU)-induced FANCD2 and Polθ foci in HeLa cells transfected with indicated siRNA. (J) Quantification of Polθ and FANCD2 localization at laser micro-irradiation sites in HeLa cells transfected with GFP-tagged full length Polθ and with indicated siRNA. Representative images are shown. Immunoblot showing siRNA-mediated CtIP knockdown efficiency. (K) Quantification of CtIP localization at laser micro-irradiation sites in FANCD2-deficient (PD20) cells expressing EV, wild-type or K561R FANCD2 cDNA construct. Data in D-K represent mean ± s.e.m. over n=3 independent experiments. Data in B-J were analyzed using Student's t test. Percentages of cells in K were analyzed using the Chi-squared test for trend in proportions. Abbreviations: ns, non significant; EV, empty vector; WT, wild-type.

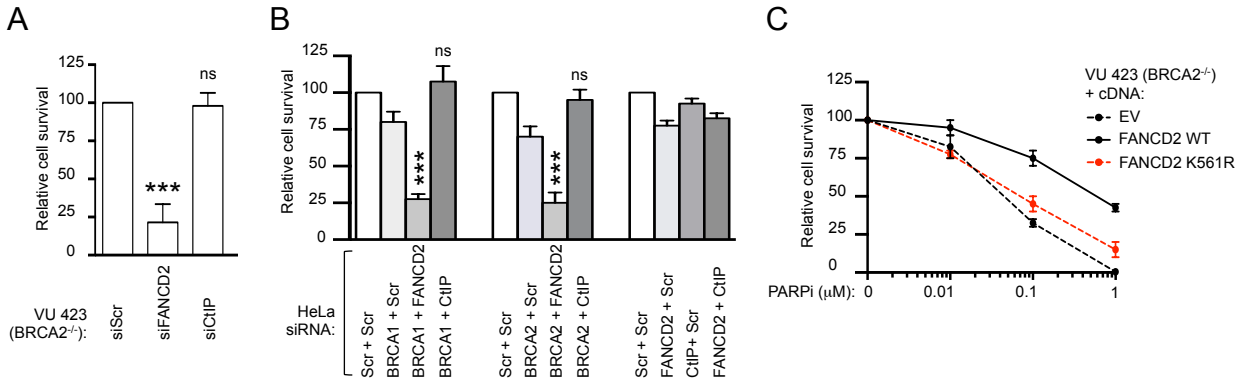

Figure S5. Related to Figures S4 and 5. CtIP depletion does not affect BRCA1/2-deficient tumor survival and FANCD2 overexpression confers resistance to PARP inhibitor in BRCA2-mutated cell line. (A) Clonogenic formation assay of BRCA2-deficient (VU 423) cells transfected with the indicated siRNA. (B) Clonogenic formation assay of HeLa cells transfected with the indicated siRNA. Percent survival is displayed as relative to siScr transfected samples, which was arbitrarily set to 100%. (C) Clonogenic formation assay of BRCA2-deficient (VU 423) cells expressing EV, wild-type or K561R FANCD2 cDNA constructs treated with increasing concentration of PARPi. Percent survival relative to non-treated cells (PARPi 0 μM) is plotted. Data in A-C represents mean ± s.e.m. over n=3 independent experiments. Data in A-B were analyzed using using the Chi-squared test for trend in proportions. Abbreviations: ns, non significant. EV, empty vector; WT, wild-type.

SUPPLEMENTAL TABLE

Cell Line name	BRCA1/2 Status	HR status
Ovarian Cancer Cell Lines		
36M2	wild-type	HRP
59M	wild-type	HRP
A1847	BRCA1 promoter hypermethylation	HRD
A2780	wild-type	HRP
BJ1	wild-type (normal fibroblast cell line)	HRP
C13	wild-type	HRP
CAOV4	wild-type	HRP
COLO720E	wild-type	HRP
COV362	BRCA1 mutation	HRD
CP70	wild-type	HRP
DOV13	wild-type	HRP
ES-2	wild-type	HRP
FUOV1	wild-type	HRP
IGROV1	wild-type	HRP
JHOS2	BRCA1 mutation	HRD
JHOS4	wild-type	HRP
KURAMOCHI	BRCA2 mutation	HRD
NIH-OVCAR3	wild-type	HRP
OAW28	wild-type	HRP
OAW42	wild-type	HRP
OV2008	wild-type	HRP
OV90	wild-type	HRP
OVCAR3	wild-type	HRP
OVCAR4	BRCA2 mutation	HRD
OVCAR420	wild-type	HRP
OVCAR5	wild-type	HRP
OVCAR8	BRCA1 promoter hypermethylation	HRD
OVKATE	wild-type	HRP
OVSAHO	BRCA2 mutation	HRD
PA-1	wild-type	HRP
PE01	BRCA2 mutation	HRD
PEO4	wild-type	HRP
RMG1	wild-type	HRP
SKOV3	wild-type	HRP
TOV21G	wild-type	HRP
TOV81D	wild-type	HRP
UWB1.289	BRCA1 mutation	HRD
WI38	wild-type (normal fibroblast cell line)	HRP
Breast Cancer Cell Lines		
BT20	wild-type	HRP
BT474	wild-type	HRP
BT549	wild-type	HRP
HCC-1143	BRCA1 mutation	HRD
HCC-1395	BRCA1 mutation	HRD
HCC-1428	wild-type	HRP

HCC-1806	wild-type	HRP
HCC-1937	BRCA1 Mutation	HRD
HCC-1954	wild-type	HRP
MCF10A	wild-type (normal breast epithelial cell line)	HRP
MCF7	wild-type	HRP
MDA-MA-436	BRCA1 Mutation	HRD
MDA-MB-231	wild-type	HRP
SKBR3	wild-type	HRP
SUM1315	BRCA1 Mutation	HRD
SUM149	BRCA1 Mutation	HRD
T47D	wild-type	HRP
ZR75-1	wild-type	HRP

Table S1. Related to Figures 3 and S3. Ovarian and breast cell lines used in the study. For each cell line, alterations (gene mutation or promoter hypermethylation) of BRCA1 and BRCA2 genes are indicated. Abbreviations: HRP (HR-proficient); HRD (HR-deficient)

SUPPLEMENTAL EXPERIMENTAL PROCEDURES

siRNAs and shRNAs

For siRNA-mediated knockdown, the following target sequences were used: BRCA1 (5'-CAGCAGUUUAUUACUCACUAATT-3'); BRCA2 (5'-GAAGAAUGCAGGUUUAAUATT-3'); FANCD2 (5'-GGAGAUUGAUGGUCUACUATT-3'); 5'UTR FANCD2 (5'-CGGCUUCUCGGAAGUAATT-3'); FANCI (5'-UCCUCAGUUUGUGCAGAUGTT-3'); USP1 (5'-UCGGCAAUACUUGCUAUCUUATT-3'); RAD52 (RAD52_7, Qiagen) and Polθ (Polθ_1, Qiagen). All siRNAs were purchased from Qiagen. AllStars negative control siRNA (Qiagen) served as the negative control. shRNAs targeting human FANCD2 was previously generated in the pTRIP/DU3-MND-GFP vector (Ceccaldi et al., 2012). ShRNAs targeting human BRCA2 (AAGAAGAATGCAGGTTTAATA), human BRCA1 (5'-AGAAUCCUAGAGAUACUGAA-3') (Pathania et al., 2011) or control (Scr, scramble) were generated in the pLKO-1 vector. Non-silencing TRIPZ-RFP doxycycline-inducible shRNA were purchased from Open Biosystems, and TRIPZ-RFP doxycycline-inducible shRNA targeting FANCD2 (5′-UACCUCAAGUGUAUCCAUG-3) was provided by Dr. A. Constantinou (Institut de Genetique Humaine, Montpellier, FR) and constructed as described in (Lossaint et al., 2013). All shRNAs were transduced upon generation of lentiviral particles.

FANCD2 cDNA

The pMMP-puro-FANCD2 wild-type and K516R constructs were previously generated in our laboratory as described (Taniguchi et al., 2002). The constructs were stably expressed in the indicated cell line by retroviral transduction and stable cells were selected using Puromycin (Sigma). The pOZ-N-Flag-HA-FANCD2 wild-type and K516R constructs were kindly provided by Dr. M. Cohn (Oxford University, UK). The constructs were expressed in the indicated cell lines by retroviral transduction and stable cells were positively selected using magnetic Dynabeads (Life Technologies) conjugated to the IL2R antibody (Millipore).

Immunofluorescence

For FANCD2 immunofluorescence experiments, cells were transfected with the indicated siRNA 48 h before treatment with HU (0.1 mM, overnight) and subsequently fixed and stained. For laser micro-irradiation experiments, cells were treated with Hoechst 33242 (0.1 μg/ml) (Thermo scientific) for 5 min, subsequently micro-irradiated with a 405 nm laser coupled to a Leica sp5 confocal laser-scanning microscope and fixed 1 h after the laser treatment. For Polθ localization to laser stripes, cells were transfected with GFP–Polθ 24 h before Hoechst 33242 treatment and subsequently micro-irradiated. The percentage of cells with Polθ at laser stripes was scored immediately after laser micro-irradiation. For GFP fluorescence, cells were grown on coverslips, treated with UV (24 h after GFP–Polθ transfection;

40 $J.m^{-2}$), and fixed 6 h after UV treatment. For colocalization studies of FANCD2, PCNA and TopBP1, cells were pre-extracted before fixation with CSK buffer complemented with 0.5% Triton X-100 as previously described (Groth et al., 2007). For all the experiments, cells were fixed with 4% paraformaldehyde for 10 min at 4°C, followed by extraction with 0.3% Triton X-100 for 10 min, washed three times with PBS and mounted with DAPI-containing mounting medium (Vector Laboratories). Primary antibody staining was performed at room temperature for 2 h followed by a secondary antibody incubation of 1 h at room temperature. Images were captured using a Zeiss AX10 fluorescence microscope and AxioVision software. Foci-positive cells were quantified by counting the number of cells with more than 10 foci. At least 150 cells were counted for each sample.

FANCD2 gene expression

The primers used for FANCD2 are as follows: (Forward: 5'-CAAACAGAATGAAGCCAGCA-3'; Reverse: 5'-CCATGGTCACAGCACCAATA-3'). For the expression data shown in Figure 3A, expression values were obtained from the CCLE collection and plotted as z-scores. The CCLE collection contains expression values for 58 breast cell lines including all the 18 breast panel cell lines tested for survival after FANCD2 inhibition with the exception of MCF10A and SUM149 cell lines. Cell lines were grouped based on their genetic status. Cell lines that did not fall into the Nle, Hormone receptor positive or TNBC groups were plotted under the group nominated as "other".

Studies of xenograft-bearing CrTac: NCr-Foxn1nu mice

The Animal Resource Facility at The Dana-Farber Cancer Institute approved all housing situations, treatments and experiments using mice. No more than five mice were housed per air-filtered cage with *ad libitum* access to standard diet and water, and were maintained in a temperature- and light-controlled animal facility under pathogen-free conditions. All mice described in this text were drug and procedure naive before the start of the experiments. For every xenograft study, we subcutaneously implanted 2.0×10^6 MDA-MB436 cells expressing either doxycycline inducible FANCD2 or scrambled shRNA (1:1 in Matrigel Matrix, BD Biosciences) into both flanks of 6–8-week-old female CrTac: NCr-Foxn1nu mice (Taconic). Doxycycline (Sigma) was added to the food (625 p.p.m.) and bi-weekly (Mondays and Thursdays) to the water (200 μg ml^{-1}) for mice bearing tumors that reached 100–200 mm^3. Tumor volumes were calculated bi-weekly using caliper measurements (length × $width^2$)/2. Growth curves were plotted as the mean tumor volume (mm^3) for each treatment group; relative tumor volume (RTV) indicates the change in tumor volume at a given time point relative to the tumor volume at the day of initial measurement (volume of approximately 0.15 cm^3) which was arbitrarily set to 1. Mice were monitored every day and euthanized by CO_2 inhalation when tumor size (≥ 2 cm), tumor status (necrosis/ulceration) or body weight loss (≥ 20%) reached ethical endpoint, according to the rules of the Animal Resource Facility at The Dana-Farber Cancer Institute.

SUPPLEMENTAL REFERENCES

Ceccaldi, R., Parmar, K., Mouly, E., Delord, M., Kim, J.M., Regairaz, M., Pla, M., Vasquez, N., Zhang, Q.S., Pondarre, C.*, et al.* (2012). Bone marrow failure in Fanconi anemia is triggered by an exacerbated p53/p21 DNA damage response that impairs hematopoietic stem and progenitor cells. Cell stem cell *11*, 36-49.

Groth, A., Corpet, A., Cook, A.J., Roche, D., Bartek, J., Lukas, J., and Almouzni, G. (2007). Regulation of replication fork progression through histone supply and demand. Science *318*, 1928-1931.

Lossaint, G., Larroque, M., Ribeyre, C., Bec, N., Larroque, C., Decaillet, C., Gari, K., and Constantinou, A. (2013). FANCD2 binds MCM proteins and controls replisome function upon activation of s phase checkpoint signaling. Molecular cell *51*, 678-690.

Pathania, S., Nguyen, J., Hill, S.J., Scully, R., Adelmant, G.O., Marto, J.A., Feunteun, J., and Livingston, D.M. (2011). BRCA1 is required for postreplication repair after UV-induced DNA damage. Molecular cell *44*, 235-251.

Taniguchi, T., Garcia-Higuera, I., Xu, B., Andreassen, P.R., Gregory, R.C., Kim, S.T., Lane, W.S., Kastan, M.B., and D'Andrea, A.D. (2002). Convergence of the fanconi anemia and ataxia telangiectasia signaling pathways. Cell *109*, 459-472.